

5877 17.4 Solutions of Exercises of Chapter 9: Weak Focusing 5878 Synchrotron

5879 9.1 Construct SATURNE I. Spin Resonances

5880 A photo of SATURNE I synchrotron can be found in Fig. 9.1. A schematic layout
5881 of the ring and 90 deg cell is given in Fig. 9.22. This figure as well as Tab. 9.1
5882 which lists the parameters of the synchrotron, will be referred to in building the
5883 SATURNE I ring in the following.

5884 (a) A model of SATURNE I synchrotron.

5885 DIPOLE is used to simulate the 90° cell dipole, data are set for a hard-edge model
5886 in this exercise (for a DIPOLE model including fringe field, refer to the ZGS case,
5887 Exercise 9.2).

5888 It is necessary to have Fig. 17.55 at hand (in addition to the users' guide), when
5889 filling up the data list under DIPOLE. Some guidance regarding these data:

- 5890 • DIPOLE is defined in a cylindrical coordinate system.
- 5891 • AT is given the value of the bending sector extent: $AT=90$ degrees. The dipole
5892 EFBs coincide with DIPOLE entrance and exit boundaries.
- 5893 • RM is given the curvature radius value, $RM = B\rho/B = 0.274426548 [\text{T m}]/$
5894 $0.03259493 [\text{T}] = 8.4193 \text{ m}$, as it fits the geometry of the optical axis around the
5895 ring. The field value matches the reference rigidity under OBJET, these are the
5896 injection energy values, 3.6 MeV, proton.
- 5897 • $ACENT=45$ deg is the reference azimuth, for the positioning of the entrance and
5898 exit EFBs. It is taken half-way of the AT range, an arbitrary choice.

5899 $KPOS=2$ allows cancelling the coordinates of particle 1 (considered here as the
5900 reference trajectory, coinciding with the optical axis around the ring) at entrance
5901 and exit of DIPOLE:

- 5902 • The entrance and exit radii in and out of the AT sector for a particle on the closed
5903 orbit (*i.e.*, a particle traveling along the design optical axis) are $RE = RS = RM$.
- 5904 • The angle TE identifies with the closed orbit angle at the entrance boundary:
5905 $TE=0$, the closed orbit is normal to the EFB. TS identifies with the closed orbit
5906 angle at the exit boundary: $TE=0$, the closed orbit is normal to the EFB.

5907 A 90 deg sector in the hard edge model is given in Tab. 17.46; note that the
5908 sector has been split in two 45 deg halves, this is in order to allow a possible
5909 insertion of a beam monitor, so requiring $AT = 45$ deg, $\omega^+ = -\omega^- = 22.5$ deg.
5910 FAISCEAU located next to DIPOLE indicates that a trajectory entering DIPOLE at
5911 radius $R = RM$, normally to the EFB (thus, $Y_0 = 0$ and $T_0 = 0$ in OBJET) exits
5912 with $Y = 0$ and $T = 0$. Data validation at this stage can be performed by comparing
5913 DIPOLE's transport matrix computed with MATRIX (Tab. 17.47), and theoretical
5914 expectations (Sect. 15.2, Eq. 15.6):

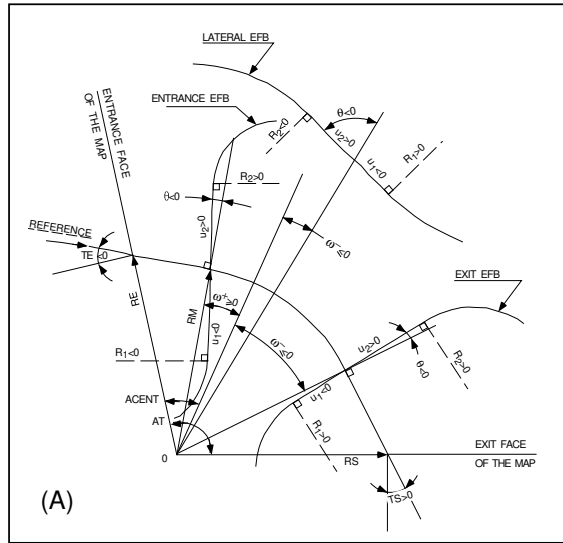


Fig. 17.55 A representation of the data that define a dipole magnet, using DIPOLE [1]

$$[T_{ij}] = \begin{matrix} \alpha = \pi/2, \\ \rho = 8.4193 \\ n = 0.6 \\ \text{(Eq. 15.6)} \end{matrix} \begin{pmatrix} 0.545794 & 11.15444 & 0 & 0 & 0 & 9.560222 \\ 0.062944 & 0.545794 & 0 & 0 & 0 & 1.324865 \\ 0 & 0 & 0.346711 & 10.19506 & 0 & 0 \\ 0 & 0 & -0.086295 & 0.346711 & 0 & 0 \\ 1.324865 & 9.560222 & 0 & 0 & 1 & 5.17640 \\ 0 & 0 & 0 & 0 & 0 & 1 \end{pmatrix} \quad (17.13)$$

5915

5916 **Introducing fringe fields**

5917 The SATURNE ring simulations which follow use the hard edge model. However, it
 5918 is leisable, at this point, to choose to add fringe fields in the model; here are the
 5919 changes which would be needed if so desired:

- 5920 • The bending sector is 90 degrees, however the field region extent AT has to
 5921 encompass the fringe fields, at both ends of the 90 deg sector. A 5 deg extension
 5922 is taken (namely, $ACENT - \omega^+ = AT - ACENT + \omega^- = 5$ deg), for a total
 5923 $AT=100$ deg which allows $RM \times \tan(ACENT - \omega^+) \approx 74$ cm; this large extension
 5924 ensures absence of truncation of the fringe fields at the AT sector boundaries,
 5925 over the all radial excursion of the beam.
- 5926 • $ACENT=50$ deg is the reference azimuth (an arbitrary value; taken half-way of
 5927 the AT range for convenience), for the positioning of the entrance and exit EFBs.
- 5928 • The entrance radius in the AT sector is $RE = RM / \cos(AT - \omega^+) = RM / \cos(5^\circ)$,
 5929 with $\omega^+ = 45$ deg the positioning of the entrance EFB with respect to $ACENT$.
 5930 And similarly for the positioning of the exit reference frame, $RS = RM / \cos(AT -$

Table 17.46 Simulation input data file: a pair of adjacent 45 degree sectors in the hard edge model. The magnet is split in order to allow insertion of FAISTORE or (here) FAISCEAU for beam monitoring. The reference optical axis has equal entrance (RE) and exit (RS) positions, and null angles (TE and TS), it coincides with the arc of radius $R = RM$ inside the sector. This input data file is named SatI_DIP.inc and defines the SATURNE I cell sequence segment S_SatI_DIP to E_SatI_DIP, for INCLUDE statements in subsequent exercises

```

File name: SatI_DIP.inc
! SATURNE I. Hard edge dipole model. Transport matrix.
'MARKER' SatI_DIP.inc_S                               ! Just for edition purposes.
'OBJET'
0.274426548e3                                         ! Reference Brho: 3.6 MeV proton.
5                                                       ! Create a 13 particle set, proper for MATRIX computation.
.001 .01 .001 .01 .001 .0001                          ! Coordinate sampling.
0. 0. 0. 0. 0. 1.                                     ! Reference trajectory: all initial coordinates nul, relative rigidity D=1.
1
'MARKER' S_SatI_DIP   ! Cell dipole begins here. A marker used for INCLUDES in subsequent exercises.

'DIPOLE' upstream_half ! Analytical modeling of a dipole magnet.
0 ! set IL=2 here, to log trajectory coordinates in zgoubi.plt, at integration steps.
45. 841.93 ! Field region angle=90; reference radius set to curvature radius value.
22.5 0. 3259493638 -0.6 0. 0. ! Reference angle ACENT set to AT/2; Bo field at RM; indices, all zero.
.0 0. ! EFB 1, hard-edged.
4 .1455 2.2670 -.6395 1.1558 0. 0. ! Enge coefficients.
22.5 0. 1.E6 -1.E6 1.E6 1.E6 ! Angle to ACENT; face angle; face is straight.
.0 0. ! EFB 2, hard-edged.
4 .1455 2.2670 -.6395 1.1558 0. 0.
-22.5 0. 1.E6 -1.E6 1.E6 1.E6
0. 0. ! EFB 3. Unused.
0 0. 0. 0. 0. 0. 0.
0 0. 1.E6 -1.E6 1.E6 1.E6 0.
2 1 ! Degree of interpolation polynomial; flying grid sizing.
2. ! Integration step size. It can be large in uniform field.
2 841.93 0. 841.93 0. ! Positioning of entrance and exit frames.
'MARKER' half-dipole !.plt ! Uncomment LABEL_2='.plt' (may go with IL=2 under DIPOLE) to
! log particle data in zgoubi.plt.
'FAISCEAU' ! Provides local coordinates, and ellipse parameters, at center of SATURNE I dipole.
'DIPOLE' downstream_half ! Analytical modeling of a dipole magnet.
0 ! set IL=2 here, to log trajectory coordinates in zgoubi.plt, at integration steps.
45. 841.93 ! Field region angle=90; reference radius set to curvature radius value.
22.5 0. 3259493638 -0.6 0. 0. ! Reference angle ACENT set to AT/2; Bo field at RM; indices, all zero.
.0 0. ! EFB 1, hard-edged.
4 .1455 2.2670 -.6395 1.1558 0. 0. ! Enge coefficients.
22.5 0. 1.E6 -1.E6 1.E6 1.E6 ! Angle to ACENT; face angle; face is straight.
.0 0. ! EFB 2, hard-edged.
4 .1455 2.2670 -.6395 1.1558 0. 0.
-22.5 0. 1.E6 -1.E6 1.E6 1.E6
0. 0. ! EFB 3. Unused.
0 0. 0. 0. 0. 0. 0.
0 0. 1.E6 -1.E6 1.E6 1.E6 0.
2 1 ! Degree of interpolation polynomial; flying grid sizing.
2. ! Integration step size. It can be large in uniform field.
2 841.93 0. 841.93 0. ! Positioning of entrance and exit frames.
'MARKER' E_SatI_DIP   ! Cell dipole ends here. A marker used for INCLUDES in subsequent exercises.
'FAISCEAU' ! Local particle coordinates.
'MATRIX' ! Compute transport matrix, from trajectory coordinates.
1 0
'MARKER' SatI_DIP.inc_E ! Just for edition purposes.
'END'

```

- 5931 $(ACENT - \omega^-) = RM/\cos(5^\circ)$ with $\omega^- = -45$ deg the positioning of the exit
- 5932 EFB. Note that $\omega^+ - \omega^- = 90^\circ$, the value of the bend angle.
- 5933 • The entrance angle TE identifies with the angular increase of the sector: TE=5 deg.
- 5934 And similarly for the positioning of exit frame, 5 deg downstream of the exit EFB,
- 5935 thus TS=5 deg.
- 5936 • Negative drifts with length $RM \times \tan(ACENT - \omega^+) = 0.7366545469$ cm need
- 5937 to be added upstream and downstream of DIPOLE, to account for the optical axis
- 5938 additional length over the 5 deg angular extent.

Table 17.47 Outcomes of the simulation file of Tab. 17.46

An excerpt from *zgoubi.res* execution listing. Coordinates of the first particle (considered here as the reference trajectory) and its path length under FAISCEAU, at OBJET on the left hand side below, locally on the right hand side:

```

3 Keyword, label(s) : FAISCEAU
                                TRACE DU FAISCEAU
                                (follows element # 2)
                                13 TRAJECTOIRES
                                OBJET
                                FAISCEAU
0 1 D Y(cm) T(mr) Z(cm) P(mr) S(cm) D-1 Y(cm) T(mr) Z(cm) P(mr) S(cm)
    1.0000 0.000 0.000 0.000 0.000 0.0000 0.0000 0.000 0.000 0.000 0.000 1.322501E+03

```

Transport matrix of SATURNE I 90 degree sector bend, in the hard edge model, two difference cases of integration step size, namely, 4 cm and 1 m (an excerpt of MATRIX computation, from *zgoubi.res* execution listing). It can be checked against matrix transport expectations. The “first order symplectic conditions” are very small in the 4 cm step size case, which is an indication of accurate numerical integration of the trajectories across DIPOLE; the reference trajectory (first one) exits better aligned (reference coordinates, before change of frame for MATRIX computation, are closer to zero):

- Case of 4 cm step size:

```

4 Keyword, label(s) : MATRIX
Reference, before change of frame (particle # 1 - D-1,Y,T,Z,s,time) :
0.00000000E+00 4.53054326E-07 6.27843350E-07 0.00000000E+00 0.00000000E+00 1.32250055E+03 4.41138700E-02

TRANSFER MATRIX ORDRE 1 (MKSA units)
0.545795 11.1544 0.00000 0.00000 0.00000 9.56022
-6.294423E-02 0.545795 0.00000 0.00000 0.00000 1.32487
0.00000 0.00000 0.346711 10.1951 0.00000 0.00000
0.00000 0.00000 -8.629576E-02 0.346711 0.00000 0.00000
1.32487 9.56022 0.00000 0.00000 1.00000 5.17640
0.00000 0.00000 0.00000 0.00000 0.00000 1.00000

DetY-1 = 0.0000000278, DetZ-1 = 0.0000000045

```

- Case of 1 m step size:

```

4 Keyword, label(s) : MATRIX
Reference, before change of frame (particle # 1 - D-1,Y,T,Z,s,time) :
0.00000000E+00 -7.54923113E-03 -1.08904867E-02 0.00000000E+00 0.00000000E+00 1.32249873E+03 4.41138091E-02

TRANSFER MATRIX ORDRE 1 (MKSA units)
0.545757 11.1567 0.00000 0.00000 0.00000 9.56154
-6.295274E-02 0.546125 0.00000 0.00000 0.00000 1.32517
0.00000 0.00000 0.346697 10.1954 0.00000 0.00000
0.00000 0.00000 -8.629900E-02 0.346750 0.00000 0.00000
1.32486 9.56148 0.00000 0.00000 1.00000 5.17692
0.00000 0.00000 0.00000 0.00000 0.00000 1.00000

DetY-1 = 0.0003978566, DetZ-1 = 0.0000685588

```

5939 (b) SATURNE I cell.

5940 A cell with origin in the middle of the drift is given Tab. 17.48, it is comprised of
5941 the split dipole and a pair of 2 m half-drifts at each ends (Fig. 9.22).

5942 *Closed orbit; chromatic closed orbit*

5943 The on-momentum closed orbit has been set to zero along the drifts ($Y_{c.o.} \equiv 0$),
5944 above, by a proper choice of RE, RS radii and TE, TS incidence angles.

Table 17.48 Simulation input data file: SATURNEI cell, assembled by INCLUDE-ing DIPOLE taken from Tab. 17.46 together with two half-drifts. This input data file is named SatI_cell.inc and defines the SATURNEI cell sequence segment S_SatI_cell to E_SatI_cell, for INCLUDE statements in subsequent exercises

```

File name: SatI_cell.inc.
! SATURNE I, one cell of the 4-period ring.
'MARKER' SatICellMATRIX_S                               ! Just for edition purposes.
'OBJET'
0.274426548e3                                           ! Reference Brho: 3.6 MeV proton.
5                                                         ! Create a 13 particle set, proper for MATRIX computation.
.001 .01 .001 .01 .001 .0001                             ! Coordinate sampling.
0. 0. 0. 0. 1.     ! Reference trajectory: all initial coordinates nul, relative rigidity D=1.

'MARKER' S_SatI_cell
'DRIFT' half_drift
200.
'INCLUDE'
1
./SatI_DIP.inc[S_SatI_DIP:E_SatI_DIP]
'DRIFT' half_drift
200.
'MARKER' E_SatI_cell
'FAISCEAU'                                               ! Local particle coordinates.
'TWISS' ! Produce transport matrix, beam matrix, and periodic optical functions along the sequence.
2 1. 1.
'MARKER' SatICellMATRIX_E                               ! Just for edition purposes.
'END'

```

The radial coordinate of an off-momentum chromatic orbit can be estimated from the dispersion, Eq. 9.26, namely,

$$Y_{\delta} = \frac{\rho_0}{1-n} \frac{\delta p}{p} = 841.93 \frac{10^{-4}}{1-(-0.6)} \approx 0.21048 \text{ cm}$$

5945 whereas the orbit angle is zero, around the ring (on- and off-momentum closed orbits
5946 are parallel to the optical axis).

5947 Besides,

5948 - computation of an accurate value of Y_{δ} is performed adding FIT at the end of
5949 the cell;

5950 - in order to raytrace three particles, respectively on-momentum and at $\delta p/p =$
5951 $\pm 10^{-4}$, OBJET[KOBJ=2] is used;

5952 - in order to raytrace around the ring, for the purpose of plotting the closed orbit
5953 coordinates, a 4-cell sequence follows the FIT procedure.

5954 This results in the input data file given in Tab. 17.49. Running this input simulation
5955 file produces the following coordinates as per the FIT procedure (an excerpt from
5956 zgoubi.res execution listing):

```

5957 STATUS OF VARIABLES (Iteration # 4 / 999 max.)
5958 LMNT VAR PARAM MINIMUM INITIAL FINAL MAXIMUM STEP NAME LBL1 LBL2
5959 2 1 30 0.168 0.211 0.21056000 0.253 1.040E-05 OBJET - -
5960 2 2 40 0.00 0.00 0.00000000 0.00 0.00 OBJET - -
5961 2 3 50 -0.253 -0.210 -0.21040403 -0.168 1.040E-05 OBJET - -
5962 STATUS OF CONSTRAINTS (Target penalty = 1.0000E-10)
5963 TYPE I J LMNT# DESIRED WEIGHT REACHED KI2 NAME LBL1 LBL2 Nb param. [value]
5964 3 1 2 12 0.0000000E+00 1.000E+00 1.466978E-06 6.70E-01 MARKER E_SatI_cell - - 0
5965 3 2 2 12 0.0000000E+00 1.000E+00 6.028957E-07 1.13E-01 MARKER E_SatI_cell - - 0
5966 3 3 2 12 0.0000000E+00 1.000E+00 8.357183E-07 2.17E-01 MARKER E_SatI_cell - - 0
5967 Fit reached penalty value 3.2139E-12

```

5968 The local coordinates Y , T and initial coordinates Y_0 , T_0 (as defined under OBJET)
5969 are identical to better than $5 \mu\text{m}$, $0.5 \mu\text{rad}$ accuracy, respectively, confirming the

5970 periodicity of these chromatic trajectories. Orbit coordinates around the ring are displayed in Fig. 17.56.

Table 17.49 Simulation input data file: first find the periodic orbit through a cell, then complete a 4-cell turn

```

SatI_Orbits.INC.dat: SATURNE I, on-momentum and chromatic orbits.
'MARKER' SatI_Orbits_S ! Just for edition purposes.
'OBJET'
0.274426548e3 ! Reference Brho: 3.6 MeV proton.
2 ! Create particles individually.
3 ! Three particles.
+.210560 0. 0. 0. 1.0001 'p' ! Chromatic orbit coordinates Y0 and T0 for D=1.001 relative rigidity.
0. 0. 0. 0. 1. 'o' ! On-momentum orbit.
-.210404 0. 0. 0. 0.9999 'm' ! Chromatic orbit coordinates Y0 and T0 for D=0.999 relative rigidity.
1 1 1

'INCLUDE'
1
./SatI_cell.inc[S_SatI_cell:E_SatI_cell]

'FIT'
2
2 30 0 .2 ! Vary Y_0(particle 1) under OBJET.
2 50 0 .2 ! Vary Y_0(particle 3) under OBJET.
2
3.1 1 2 #End 0. 1. 0 ! Constrain Y(particle 1)=Y_0(particle 1).
3.1 3 2 #End 0. 1. 0 ! Constrain Y(particle 1)=Y_0(particle 1).

! When FIT is done converging on the constraints, execution quietly carries on with the periodic
! coordinates , raytracing through 4 cells to complete a turn around the ring.
'INCLUDE'
1
4 * ./SatI_cell.inc[S_SatI_cell:E_SatI_cell]

'SYSTEM'
1
gnuplot < gnuplot_Zplt_traj.gnu ! Plot the orbit radial coordiante.
'MARKER' SatI_Orbits_E ! Just for edition purposes.
'END'

```

A gnuplot script (excerpt) to obtain a graph of particle coordinates, from zgoubi.plt (as in Fig. 17.56):

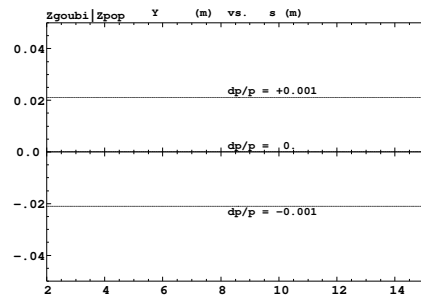
```

# gnuplot_Zplt_traj.gnu
traj1 = 1 ; traj2 = 3
plot \
for [i=traj1:traj2] 'zgoubi.plt' u ($19== i ? $14 *cm2m : 1/0):($10 *cm2m):($19) w p ps .4 lc palette

```

5971

Fig. 17.56 Radial coordinate of the orbits around the ring, on-momentum, and for $dp/p = \pm 10^{-3}$. A graph obtained using zpop, data read from zgoubi.plt: menu 7; 1/1 to open zgoubi.plt; 2/[6,2] for Y versus distance s; 7 to plot. A gnuplot script for a similar graph given is given in Tab. 17.49



5972 *Lattice parameters*

5973 The TWISS command down the sequence (Tab. 17.48) produces the periodic beam matrix results shown in Tab. 17.50; MATRIX[IFOC=11] would, as well. It also

Table 17.50 Results obtained running the simulation input data file of Tab. 17.48, SATURNEI cell - an excerpt from zgoubi.res execution listing

```

14 Keyword, label(s) : TWISS
Reference, before change of frame (particle # 1 - D-I,Y,T,Z,s,time) :
0.00000000E+00 6.02895730E-07 6.54169939E-07 0.00000000E+00 0.00000000E+00 1.72250055E+03 6.57784696E-01

Beam matrix (beta/-alpha/-alpha/gamma) and periodic dispersion (MKSA units)
14.418595 0.000000 0.000000 0.000000 0.000000 21.048250
0.000000 0.069355 0.000000 0.000000 0.000000 0.000000
0.000000 0.000000 11.411041 0.000000 0.000000 -0.000000
0.000000 0.000000 0.000000 0.087634 0.000000 0.000000
0.000000 0.000000 0.000000 0.000000 0.000000 0.000000
0.000000 0.000000 0.000000 0.000000 0.000000 0.000000

Betatron tunes (Q1 Q2 modes)
NU_Y = 0.18103144 NU_Z = 0.22214599

dL/L / dp/p = 1.9194487
(dp = 0.000000E+00 L(0) = 1.72250E+03 cm, L(0)-L(-dp) = 3.30606E-01 cm, L(0)-L(+dp) = -3.30645E-01 cm)

Transition gamma = 7.21791469E-01

Chromaticities :
dNu_y / dp/p = -0.60221729 dNu_z / dp/p = 0.38005442

```

5974

5975 produces a zgoubi.TWISS.out file which details the optical functions along the
5976 sequence (at the downstream end of the optical elements). The header of that file
5977 details the optical parameters of the structure (Tab. 17.51).

Table 17.51 An excerpt of zgoubi.TWISS.out file resulting from the execution of the SATURNEI cell simulation input data file of Tab. 17.48. Note that the ring (4-period) wave numbers are 4 times the cell values Q1, Q2 displayed here. Optical functions (betatron function and derivative, orbit, phase advance, etc.) along the optical sequence are listed as part of zgoubi.TWISS.out following th header. The top part and last line of that listing are given below

```
@ LENGTH      %le 17.22500552
@ ALFA        %le 1.919448707
@ ORBITS      %le -0
@ GAMMATR     %le 0.7217914685
@ Q1          %le 0.1810314404 [fractional]
@ Q2          %le 0.2221459901 [fractional]
@ DQ1        %le -0.6022172911
@ DQ2        %le 0.3800544183
@ DXMAX      %le 2.10586311E+01 @ DXMIN      %le 2.10482503E+01
@ DYMAX      %le 0.00000000E+00 @ DYMIN      %le 0.00000000E+00
@ XCOMAX     %le 2.10528899E-01 @ XCOMIN     %le 0.00000000E+00
@ YCOMAX     %le 0.00000000E+00 @ YCOMIN     %le 0.00000000E+00
@ BETMAX     %le 1.57006971E+01 @ BETXMIN    %le 1.44132839E+01
@ BETYMAX    %le 1.30884296E+01 @ BETYMIN    %le 1.14110171E+01
@ XCORMS     %le 6.05227342E-04
@ YCORMS     %le 0. not computed
@ DXRMS      %le 2.98427468E-03
@ DYRMS      %le 0.00000000E+00
```

Optical functions listing zgoubi.TWISS.out (there is more: $D_{x,y}$, etc.: lines are truncated, here), including the periodic $\alpha_{x,y,l}$, $\beta_{x,y,l}$, $D_{x,y}$, etc.

```
# alfx      btx      alfy      bty      alfl      bt1      Dx      Dxp
# 1         2         3         4         5         6         7         8
1.3683565E-08 1.4426805E+01 -6.6336606E-09 1.1411067E+01 0.0000000E+00 0.0000000E+00 2.1058631E+01 1.1261490E-03
2.3958789E-08 1.4426805E+01 -2.0952612E-10 1.1411067E+01 0.0000000E+00 0.0000000E+00 2.1048250E+01 3.4685148E-09
2.3958789E-08 1.4426805E+01 -2.0952612E-10 1.1411067E+01 0.0000000E+00 0.0000000E+00 2.1048250E+01 3.4685148E-09
-1.3863081E-01 1.4704066E-01 -1.7526845E-01 1.1761604E+01 0.0000000E+00 0.0000000E+00 2.1048250E+01 3.4685148E-09
-1.3863081E-01 1.4704066E-01 -1.7526845E-01 1.1761604E+01 0.0000000E+00 0.0000000E+00 2.1048250E+01 3.4685148E-09
5.1661104E-04 1.5700697E-01 2.2204071E-06 1.3088430E+01 0.0000000E+00 0.0000000E+00 2.1048250E+01 1.4621225E-09
5.1661104E-04 1.5700697E-01 2.2204071E-06 1.3088430E+01 0.0000000E+00 0.0000000E+00 2.1048250E+01 1.4621225E-09
1.3919474E-01 1.4692541E-01 1.7526999E-01 1.1761559E+01 0.0000000E+00 0.0000000E+00 2.1048250E+01 3.4685146E-09
1.3919474E-01 1.4692541E-01 1.7526999E-01 1.1761559E+01 0.0000000E+00 0.0000000E+00 2.1048250E+01 3.4685146E-09
4.3383067E-04 1.4413284E+01 7.7310157E-07 1.1411017E+01 0.0000000E+00 0.0000000E+00 2.1048250E+01 3.4685146E-09
4.3383067E-04 1.4413284E+01 7.7310157E-07 1.1411017E+01 0.0000000E+00 0.0000000E+00 2.1048250E+01 3.4685146E-09
```

5978 *Moving the origin of the cell*

5979 The origin of the sequence can be moved by placing both drifts on one side of
5980 DIPOLE. It can also be taken in the middle of DIPOLE, as the latter has been split.
5981 A fully deployed input data sequence (INCLUDEs accounted for) is provided at the
5982 top of the execution listing zgoubi.res, it can be used to copy-paste pieces around.
5983 It can then be checked that betatron tunes, chromaticities, momentum compaction
5984 (Tab. 17.50) do not change, and that the beam matrix does.

5985 *Optical functions along the cell*

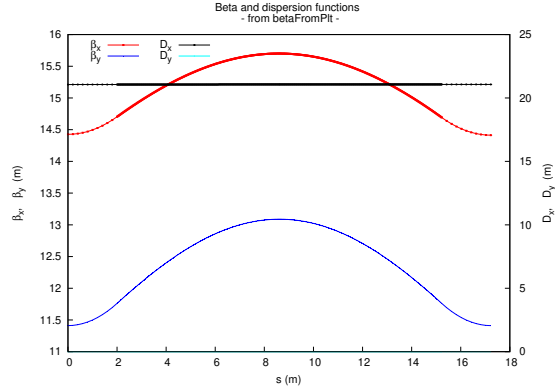
They are computed by transporting the beam matrix, from the origin. A Fortran program available in zgoubi sourceforge package toolbox, betaFromPlt [1], performs this computation in the following way: OBJET[KOBJ=5.1] provides the initial beta function values (determined in the previous question); IL=2 under DIPOLE logs stepwise particle data in zgoubi.plt; 'split 10 2' added under DRIFT does it, too. The program betaFromPlt computes the transport matrix T_{step_i} from the origin of the sequence (at OBJET) to the considered step_i along the sequence, using particle

coordinates read in zgoubi.plt - a similar computation to what MATRIX does [1, MATRIX Sect.]. The beam matrix $\sigma = \begin{bmatrix} \beta & -\alpha \\ -\alpha & \gamma \end{bmatrix}$ is then transported, from the origin to step_i, using (Eq. 16.10)

$$\sigma_{\text{step}_i} = T_{\text{step}_i} \sigma_{\text{origin}} \tilde{T}_{\text{step}_i}$$

The result is displayed in Fig. 17.57.

Fig. 17.57 Optical functions along SATURNE I cell. They are obtained from the transport of the beta functions, from the origin (at OBJET), using transport matrices computed from step-by-step particle coordinates stored in zgoubi.plt



5986

5987 *Tune scan*

5988 A simulation is given in Tab. 17.52, derived from Tab. 17.48: MATRIX[IFOC=11]
 5989 has been substituted to TWISS, a REBELOTE do loop repeatedly changes *n*. A
 5990 graph of the scan is given in Fig. 17.58, a few values are detailed in Tab. 17.53.

Fig. 17.58 A scan of the wave numbers, and of $\sqrt{v_Y^2 + v_Z^2} \approx \sqrt{R/\rho_0} = 1.141$, in SATURNE I for $0.5 \leq n \leq 0.757$. Solid curves are from theoretical approximations (Eq. 9.18), markers are from numerical simulations

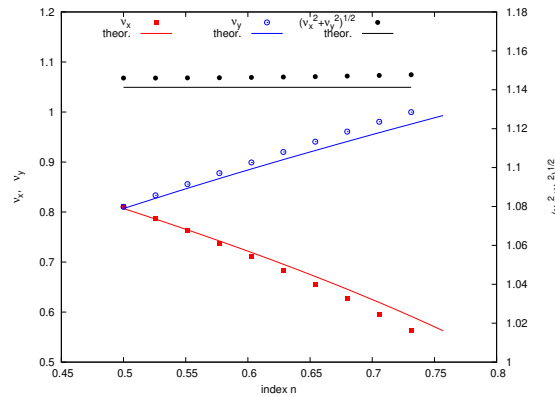


Table 17.52 Simulation input data file: tune scan, using REBELOTE to repeatedly change n . Beam matrix and wave numbers are computed by MATRIX, from the coordinates of the 13 particle sample generated by OBJET[KOBJ=5]

```

SATURNE I, tune scan.
'MARKER' SatI_Qscan_S                               ! Just for edition purposes.
'OBJET'
0.274426548e3                                       ! Reference Brho: 3.6 MeV proton.
5                                                       ! Create a 13 particle set, proper for MATRIX computation.
.001 .01 .001 .01 .001 .0001                          ! Coordinate sampling.
0. 0. 0. 0. 0. 1.                                     ! Reference trajectory: all initial coordinates nul, relative rigidity D=1.
1

'MARKER' S_SatI_cell
'DRIFT' half_drift
200.
'INCLUDE'
1
./SatI_DIP.inc[S_SatI_DIP:E_SatI_DIP]
'DRIFT' half_drift
200.
'MARKER' E_SatI_cell
'FAISCCEAU'                                           ! Local particle coordinates.
'MATRIX'
1 11 PRINT ! Comoute a 10+4 period transport matrix, and tunes. Save outcomes to zgoubi.MATRIX.out.

'REBELOTE'                                           ! A do loop: repeat the section above commencing at the top of the file,
10 1.1 0 1                                           ! 10 times.
1
DIPOLE 6 -0.757;-0.5 ! Change the value of parameter 30 (namely, n) in DIPOLE (prior to repeating).
! in any DIPOLE in the sequence.

'SYSTEM'
1
gnuplot <./gnuplot_MATRIX_Qxy.gnu                    ! Plot tunes vs index.
'MARKER' SatI_Qscan_E                               ! Just for edition purposes.
'END'

```

gnuplot script to obtain Fig. 17.58:

```

# ./gnuplot_MATRIX_Qxy.gnu
set xlabel "index n";set ylabel "{/Symbol n}_x,    ({/Symbol n}_x^2+{/Symbol n}_y^2)^{1/2}"
set ylabel "{/Symbol n}_y"; set xtics; set ytics nomirror; set y2tics nomirror; ncell=4
set key t l; set key maxrow 2; set yrange [:1.3]; set y2range [:1.06]
n1 = -0.757; dn=(.757-.5)/10.; R=10.9658; rho=8.4193
plot \
"zgoubi.MATRIX.out" u (n1+(561-1)*dn): \
($61>1? $56 *ncell :1/0) w p pt 5 lt 1 lw .5 lc rgb "red"          tit "{/Symbol n}_x " ,\
"zgoubi.MATRIX.out" u (n1+(561-1)*dn):($61>1? sqrt((1+(n1+(561-1)*dn))*R/rho): \
1/0) w l lt 1 lc rgb "red" tit "theor. " ,\
"zgoubi.MATRIX.out" u (n1+(561-1)*dn): \
($61>1? $57 *ncell :1/0) axes xly2 w p pt 6 lt 3 lw .5 lc rgb "blue"  tit "{/Symbol n}_y " ,\
"zgoubi.MATRIX.out" u (n1+(561-1)*dn): \
($61>1? sqrt(-(n1+(561-1)*dn))*R/rho):1/0) axes x2y2 w l lt 3 lc rgb "blue" tit "theor. " ,\
"zgoubi.MATRIX.out" u (n1+(561-1)*dn): \
($61>1? sqrt($56**2+$57**2) *ncell :1/0) w p pt 7 lt 1 lc rgb "black" tit "{/Symbol n}_x^2+{/Symbol n}_y^2)^{1/2}" ,\
"zgoubi.MATRIX.out" u (n1+(561-1)*dn):($61>1? sqrt(R/rho):1/0) w l lt 1 lc rgb "black" tit "theor. "
pause 1

```

Table 17.53 Dependence of wave numbers on index n , from numerical raytracing (columns denoted “ray-tr.”) and from theory

n	ν_Y		ν_Z	
	ray-tr.	$\sqrt{(1-n)\frac{R}{\rho_0}}$	ray-tr.	$\sqrt{n\frac{R}{\rho_0}}$
0.5	0.810353	0.806987	0.810353	0.806987
0.6	0.724125	0.721791	0.888583	0.884010
0.7	0.626561	0.625089	0.960806	0.954840
0.757	0.563635	0.562580	0.999804	0.992955

(c) Sinusoidal approximation of the betatron motion.

The approximation

$$y(\theta) = A \cos(\nu_Z \theta + \phi)$$

5992 is checked here considering the vertical motion (considering the horizontal motion
5993 leads to similar conclusions). The value of the various parameters in that expression
5994 are determined as follows:

- the particle raytraced for comparison is launched with an initial excursion $Z_0(\theta = 0) = 5$ cm (4th particle in OBJET, above). At the launch point (middle of the drift) the beam ellipse is upright (Fig. 17.61), whereas phase space motion is clockwise, thus take

$$A = 5 \text{ cm} \quad \text{and} \quad \phi = \pi/2$$

- the vertical betatron of the 4-cell ring tune is (Tab. 17.51)

$$\nu_Z = 4 \times 0.222146 = 0.888284$$

- $\theta = s/R$ and $R = \oint ds/2\pi$ with (Tab. 17.51)

$$2\pi R = \text{circumference} = 2\pi \times 10.9658 = 68.9 \text{ m}$$

5995 The comparison with a trajectory obtained from raytracing is given in Fig. 17.59
5996 and confirms the validity of the sinusoidal approximation.

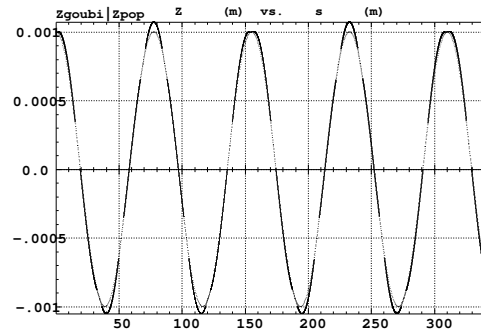


Fig. 17.59 Vertical betatron motion, five turns around SAT-URNEI ring, from raytracing (modulated oscillation), and sine approximation, superimposed

5997 (d) Beam envelopes.

5998 A few particles are launched through the cell with initial coordinates taken on a
5999 common invariant (horizontal and/or vertical), using OBJET[KOBJ=8]. The input
6000 data file is given in Tab. 17.54. The initial ellipse parameters (under OBJET) are
6001 the periodic values $\alpha_Y = \alpha_Z = 0$, $\beta_Y = 14.426$ m, $\beta_Z = 11.411$ m, found in
6002 zgoubi.TWISS.out (Tab. 17.51). The envelopes so generated, and the quantities
6003 $u^2(s)/\varepsilon_u/\pi$ (Eq. 9.23), are displayed in Fig. 17.60. The extremum extremorum
6004 value of $u^2(s)/\varepsilon_u/\pi$ comes out to be, respectively, $\hat{\beta}_Y = 14.4$ m and $\hat{\beta}_Z = 15.7$ m,
6005 consistent with earlier derivations (BETXMAX and BETYMAX values in Tab. 17.51
6006 and Fig. 17.57).

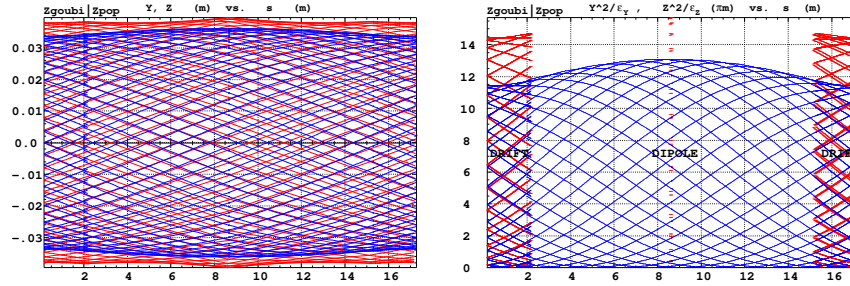


Fig. 17.60 Left: horizontal and vertical envelopes as generated by plotting the coordinates $Y(s)$ (greater excursion, red, along the drifts and dipole) or $Z(s)$ (smaller excursion, blue) across the SATURNE I cell, of 60 particles evenly distributed on a common $10^{-4} \pi$ m invariant, either horizontal or vertical (while the other invariant is zero). Right: a plot of $Y^2(s)/\epsilon_Y/\pi$ and $Z^2(s)/\epsilon_Z/\pi$; their extrema identify with $\beta_Y(s)$ and $\beta_Z(s)$, respectively. Graphs obtained using zpop, data read from zgoubi.plt: menu 7; 1/5 to open zgoubi.fai; 2/[6,2] (or [6,4]) for Y versus s (or Z versus s); 7 to plot; option 3/14 to raise Y (or Z) to the square

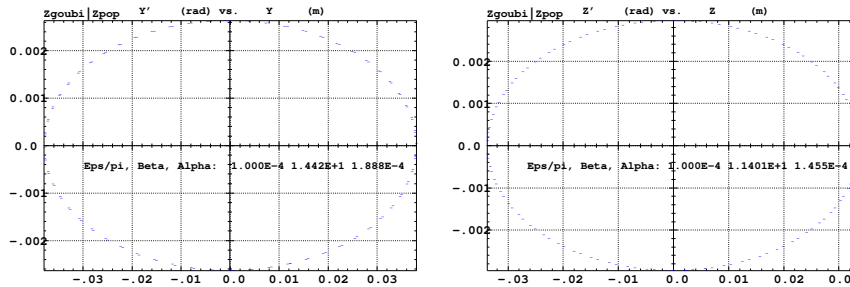


Fig. 17.61 Sixty particles evenly distributed on a common periodic invariant (either $\epsilon_Y = 10^{-4} \pi$ m and $\epsilon_Z = 0$, left graph, or the reverse, right graph) have been tracked through the cell. Initial and final phase space coordinates are displayed in these graphs: the initial and final ellipses which initial and final particle positions lie on superimpose. Optical function values given in the figures result from an *rms* match, of indifferently the initial or final coordinates; they do agree with the TWISS data (Tab.17.51). A graph obtained using zpop, data read from zgoubi.fai: menu 7; 1/5 to open zgoubi.fai; 2/[2,3] (or [4,5]) for T versus Y (or P versus Z); 7 to plot

6011 (e) An acceleration cycle. Symplecticity checks.

Eleven particles are launched for a 30,000 turn tracking at a rate of

$$\Delta W = q\hat{V} \cos \phi_s = 200 \times \sin 150^\circ = 100 \text{ keV/turn}$$

6012 ($E : 3.6 \rightarrow 3.0036 \text{ GeV}$), all evenly distributed on the same initial vertical invariant

$$Z^2/\beta_Z + \beta_Z Z'^2 = \epsilon_Z/\pi \tag{17.14}$$

6013 with $\epsilon_Z/\pi = 10^{-4} \text{ m}$, or, normalized, $\beta_Y \epsilon_Z/\pi = 0.08768 \times 10^{-4} \text{ m}$.

The simulation file is given in Tab. 17.55. CAVITE[IOPT=3] is used, it provides an RF phase independent boost

$$\Delta W = q\hat{V} \sin \phi_s$$

6014 as including synchrotron motion is not necessary here, even better, this ensures
 6015 constant depolarizing resonance crossing speed, so precluding any possibility of
 6016 multiple crossing (it can be referred to [3] regarding that effect).

Table 17.55 Simulation input data file: track 11 particles launched on the same vertical invariant. The INCLUDE adds the SATURNE I cell four times, the latter is defined in Tab. 17.48 and Fig. 9.22

```

SATURNE I ring. Polarization landscape.
'MARKER' SatIPolarLand_S ! Just for edition purposes.
'OBJET'
0.274426548e3 ! Reference Brho: 3.6 MeV proton.
8 ! Create a set of 60 particles evenly distributed on the same invariant;
1 11 1 ! case of 11 particles on a vertical invariant; use 11 1 1 instead for horizontal invariant.
0. 0. 0. 0. 0. 1.
0. 14.426 1e-4 ! Periodic optical functions and invariant value, horizontal and
0. 11.411 1e-4 ! vertical.
0. 1. 0. ! No momentum spread.

'MCOBJET' ! Commented.
!1.03527036749193e3 ! Reference Brho: 50 MeV proton.
!3 ! Create a 13 particle set, proper for MATRIX computation.
!200
!2 2 2 2 2 2
!0. 0. 0. 0. 0. 1.
!0. 14.426 25e-6 3 ! Periodic alpha_Y, beta_Y, and invariant value;
!0. 11.411 10e-6 3 ! Periodic alpha_Z, beta_Z, and invariant value.
!0. 1. 1.e-8 3
!123456 234567 345678

'PARTICUL'
PROTON ! Necessary data in order to allow (i) spin tracking and, and (ii) acceleration.
'SPNTRK' ! Switch on spin tracking.
3 ! all initial spins vertical.
'FAISCEAU'
'FAISTORE'
b_polarLand.fai ! Log particle data in b_polarLand.fai, turn-by-turn; "b_" imposes
7 ! binary write, which results in faster i/o.

'SCALING'
1 1
DIPOLE
-1 ! Causes field increase in DIPOLE, in correlation to particle
1. ! rigidity increase by CAVITE.
1

! 4 cells follow.
'INCLUDE'
1
4* ./SatI_cell.inc[S_SatI_cell:E_SatI_cell]

'CAVITE'
3
0 0
200e3 0.523598775598 ! Acceleration rate is 200*0.5=100keV/turn.
! 20e3 0.523598775598 ! Commented: an acceleration rate of 20*0.5=10keV/turn.

'REBELOTE'
30000 0.2 99 ! Case of 100 keV/turn: ~30,000 turns from 3.6 MeV to 3 GeV.
! 300000 0.3 99 ! Commented: case of 10 keV/turn: ~300,000 turns from 3.6 MeV to 3 GeV.

'FAISCEAU'
'MARKER' SatIPolarLand_E ! Just for edition purposes.
'SPNPRT'

'END'

```

6017 *Betatron damping*

6018 Figure 17.62 shows the damped vertical motion of the individual particles, over
 6019 the acceleration range, together with the initial and final distributions of the 11
 6020 particles on elliptical invariants. Departure from the matching ellipse at the end of
 6021 the acceleration cycle, 3 GeV (Eq. 17.14 with $\varepsilon_Z/\pi = 1.0745 \times 10^{-6}$ m), is marginal.

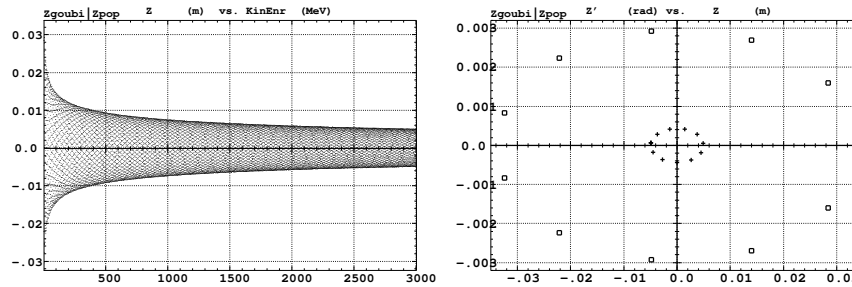
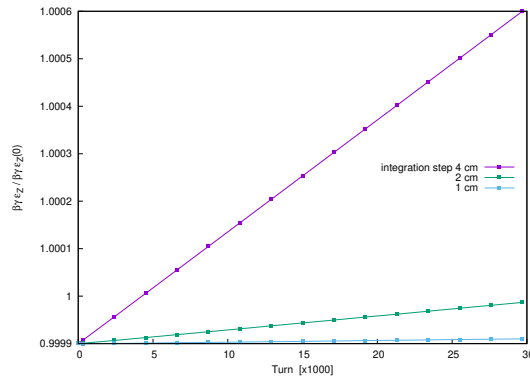


Fig. 17.62 Left: damped vertical motion, from 3.6 MeV to 3.004 GeV in 30,000 turns. Right: the initial coordinates of the 11 particles (squares) are taken on a common invariant $\varepsilon_Z(0) = 10^{-4} \pi \text{ m}$ (at 3.6 MeV, $\beta\gamma = 0.0877$, thus $\beta\gamma\varepsilon_Z(0) = 8.77 \times 10^{-6} \pi \text{ m}$); the final coordinates after 30,000 turns (crosses) appear to still be (with negligible departure) on a common invariant, of value $\varepsilon_Z(\text{final}) = 2.149 \times 10^{-6} \pi \text{ m}$ (at 3.004 GeV, $\beta\gamma = 4.08045$) or $\beta\gamma\varepsilon_Z(\text{final}) = 8.77 \times 10^{-6} \pi \text{ m}$, equal to the initial value $\beta\gamma\varepsilon_Z(0)$

6022 *Degree of non-symplecticity of the numerical integration*

6023 The degree of non-symplecticity as a function of integration step size is illustrated
 6024 in Fig. 17.63. The initial motion is taken paraxial, vertical motion is considered as
 6025 it resorts to off-mid plane Taylor expansion of fields [1, DIPOLE Sect.], a stringent
 6026 test as the latter is expected to deteriorate further the non-symplecticity inherent
 6027 to the Lorentz equation integration method (a truncated Taylor series method [1,
 6028 Eq. 1.2.4]).

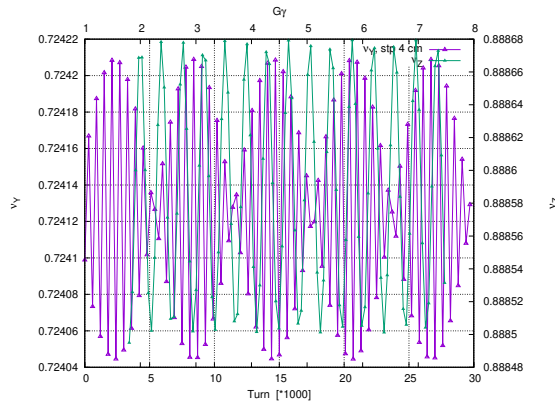
Fig. 17.63 Turn-by-turn evolution of the normalized invariant, $\beta\gamma\epsilon_Z(\text{turn})/\beta\gamma\epsilon_Z(0)$ (initial $\epsilon_Z(0)$ taken paraxial), for four different integration step size values: 1, 2 and 4 cm



6029 *Evolution of the wave numbers*

6030 The Fortran tool tunesFromFai_iterate can be used to computes tunes as a function
 6031 of turn number or energy, it reads turn-by-turn particle data from zgoubi.fai and
 6032 computes a discrete Fourier transform over so many turns (a few tens, 100 here
 6033 for instance), every so many turns (300, here) [4]. Typical results are displayed in
 6034 Fig. 17.64, tunes have the expected values: $\nu_Y = 0.7241$, $\nu_Z = 0.8885$. In acceleration
 6035 rate of 100 keV/turn has been taken (namely, $\hat{V} = 200$ kV and still $\phi_s = 150^\circ$), to
 6036 save on computing time. SCALING with option NTIM=-1 causes the magnet field
 6037 to strictly follow the momentum boost by CAVITE.

Fig. 17.64 Horizontal ring tune (left vertical axis), $\nu_Y \approx 0.7241$, and vertical ring tune (right vertical axis), $\nu_Z \approx 0.8885$, as a function of turn number, over 30,000 turns ($E : 0.0036 \rightarrow 3$ GeV at a rate of 100 keV/turn)



- 6038 (f) Crossing an isolated intrinsic depolarizing resonance.
 6039 The simulation uses the input data file of Tab. 17.55, with the following changes:
 6040 • Under OBJET:

- 6041 – 1st line, change the reference rigidity BORO for an initial $G\gamma \approx 2.95$, upstream
- 6042 of $G\gamma_R = 4 - \nu_Z \approx 3.1$,
- 6043 – 3rd line, request a single particle (“1 1 1”, in lieu of 11, “1 11 1”),
- 6044 – 6th line, set the invariant ε_Z/π to the desired value, ε_Y/π value is indifferent;
- 6045 resulting OBJET:

```

6046         'OBJET'
6047         4.08897740024e3          ! Reference Brho -> G*gamma=2.949312341 -> 605.22655 MeV proton.
6048         8                        ! Create a (set of) particle(s) on a given invariant.
6049         1 1 1                    ! case of 1 particle.
6050         0. 0. 0. 0. 0. 1.
6051         0. 1. 0.                  ! Horizontal invariant taken zero.
6052         0. 11.411 1e-4           ! Periodic alpha_Z, beta_Z, and invariant value.
6053         0. 1. 0.                ! No momentum spread.
    
```

- 6054 • change the field value under DIPOLE consistently with the new BORO value, so
- 6055 to maintain a curvature radius $\rho_0 = BORO/B = 8.4193$ m (Tab. 9.1),
- 6056 • under CAVITE, set the peak voltage to the required value,
- 6057 • under REBELOTE, set the number of turns to an appropriate value: a total of
- 6058 15,000, of which 8,000 about upstream of the resonance, is convenient for an
- 6059 acceleration rate of 10 keV/turn.

6060 *Changing the particle invariant value*

6061 Particle spin motion through the isolated resonance for seven different invariant

6062 values, $\varepsilon_Z/\pi = 1, 2, 10, 20, 40, 80, 200 \mu\text{m}$, observed at the beginning of the

6063 optical sequence (FAISTORE[b_polarLand.fai] location, Tab. 17.55), is displayed in

6064 Fig.17.65.

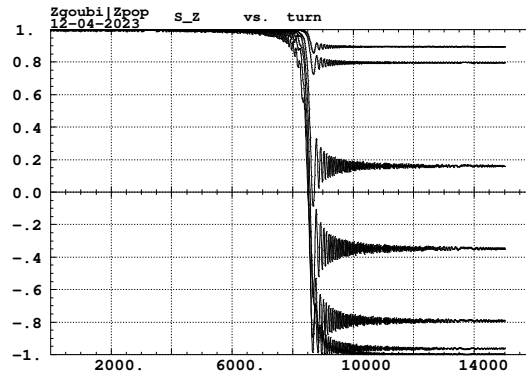


Fig. 17.65 Turn-by-turn spin motion through the isolated resonance $G\gamma_R = 4 - \nu_Z$, for 7 different values of the particle invariant from (top to bottom) $1 \mu\text{m}$ to $200 \mu\text{m}$ where full spin flip occurs. A graph obtained using zpop, data read from b_polarLand.fai; menu 7; 1/8 to open b_polarLand.fai; 2/[39,23] for S_Z versus turn; 7 to plot

6065 The intrinsic resonance strength satisfies $|\varepsilon_R|^2 = A \varepsilon_Z$, with A a factor which char-

6066 acterizes the lattice. On the other hand, from the Froissart-Stora formula (Eq. 9.39)

6067 one gets

$$|\varepsilon_R|^2 = \frac{2\alpha}{\pi} \ln \left(\frac{2}{1 + S_{Z,f}/S_{Z,i}} \right) \xrightarrow{S_{Z,f} \approx S_{Z,i}} \frac{\alpha}{\pi} \left(1 - \frac{S_{Z,f}}{S_{Z,i}} \right) \quad (17.15)$$

6068 with α , crossing speed, a constant. Thus one expects to find $\frac{1}{\varepsilon_Z} \ln \left(\frac{2}{1+S_{Z,f}/S_{Z,i}} \right)$ con-
6069 stant.

6070 Calculation of the resonance strength from the P_f/P_i tracking results, using
6071 Eq. 17.15, requires the value of the crossing speed, which is

$$\alpha = \frac{1}{2\pi} \frac{\Delta E}{M} = \frac{1}{2\pi} \frac{20 \times 10^3 \times \sin 30^\circ [\text{eV/turn}]}{938.27208 \times 10^6 [\text{eV}]} = 1.696 \times 10^{-6} \quad (17.16)$$

6072 Table 17.56, rightmost column, displays the ratio $|\epsilon_R|^2/\varepsilon_Z/\pi$ so obtained, essentially
constant as expected.

Table 17.56 Relationship between the invariant value ε_Z/π and the quantity $\ln \left(\frac{2}{1+S_{Z,f}/S_{Z,i}} \right) \propto |\epsilon_R|^2$ (Eq. 17.15). $\hat{V} = 20$ kV, here, crossing speed $\alpha = 1.696 \times 10^{-6}$ (Eq. 17.16). $S_{Z,i} = 1$ always, and $S_{Z,f}$ (col. 2) is a rough estimate from Fig. 17.65. The rightmost column gives the resulting ratio $|\epsilon_R|^2/\varepsilon_Z/\pi$, essentially constant

ε_Z/π (μm)	$\frac{S_{Z,f}}{S_{Z,i}} \equiv S_{Z,f}$	$\ln \frac{2}{1+S_{Z,f}}$	$\frac{ \epsilon_R ^2}{\varepsilon_Z/\pi}$ ($\times 10^{-8}$)
1	0.89	0.024568	2.652645
2	0.795	0.046965	2.535451
10	0.17	0.232844	2.514034
20	-0.35	0.488116	2.635115
40	-0.78	0.958607	2.587537
80	-0.975	1.903089	2.568474

6073

6074 *Changing the crossing speed*

6075 The crossing speed is reduced by a factor of 2, using $\hat{V} = 10$ kV, and accordingly
6076 the number of turns is doubled, to 30,000, the only modifications to the input data
6077 simulation file used in the previous question. Tracking results, Tab. 17.57, show that

6078 $\frac{\hat{V}}{\varepsilon_Z/\pi} \times \ln \left(\frac{2}{1+S_{Z,f}/S_{Z,i}} \right)$ is constant, as expected.

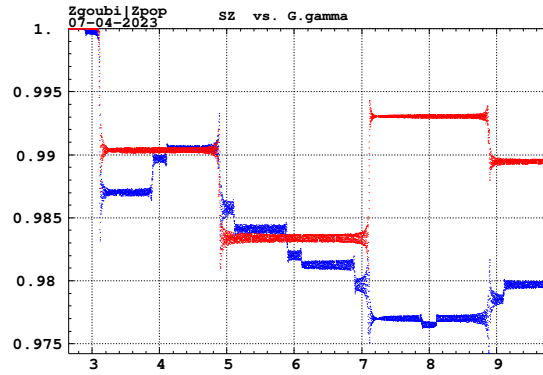
Table 17.57 Relationship between the acceleration rate $\Delta E \propto \hat{V}$ and the quantity $\ln\left(\frac{2}{1+S_{Z,t}/S_{Z,i}}\right)$. Normalized to ε_Z/π , their product (rightmost column) appears to be essentially constant, this is the expected result

ε_Z/π (μm)	\hat{V} (kV)	$\frac{S_{Z,t}}{S_{Z,i}} \equiv S_{Z,t}$	$\ln \frac{2}{1+S_{Z,t}}$	$\frac{\hat{V}}{\varepsilon_Z/\pi} \times \ln \frac{2}{1+S_{Z,t}}$
1	10	+0.79	0.048	0.482
10	10	-0.33	0.475	0.475
20	10	-0.78	0.959	0.479
1	20	+0.89	0.025	0.49
2	20	+0.795	0.047	0.47

6079 *Systematic resonances, random resonances*

6080 A single-particle tracking is pushed beyond $G\gamma = 8 + \nu_Z \approx 8.89$, 40,000 turns at
 6081 a rate of 100 kV/turn. The resulting $S_Z(G\gamma)$, Fig. 17.66, shows that in a 4-periodic
 6082 lattice the sole systematic resonances are excited, whereas all resonances are excited
 6083 if the 4-periodicity is broken - here, by changing the index to $n = -0.66$ in one
 DIPOLE, the periodicity is 1.

Fig. 17.66 Resonance crossing in SATURNE I, a turn-by-turn record of $S_Z(G\gamma)$. Case of systematic resonances $G\gamma = 4k \pm \nu_Z$ in a 4-period lattice (red), and of random resonances $G\gamma = k \pm \nu_Z$ in a 1-periodic perturbed optics lattice (blue). A graph obtained using zpop, data read from b_polarLand.fai: menu 7; 1/8 to open b_polarLand.fai; 2/[59,23] for S_Z versus $G\gamma$; 7 to plot



6084

(g) Spin motion across a weak depolarizing resonance.

6085
 6086 The goal is to check numerical outcomes against the Fresnel integral model
 6087 (Eq. 9.41). A weak resonance is obtained using small amplitude vertical motion and
 6088 fast crossing.

6089 A single particle is raytraced, in the following conditions:

- 6090 - resonance to be crossed: $G\gamma_R = 4 - \nu_y \approx 3.1115$,
- 6091 - acceleration: peak voltage $\hat{V} = 100$ kV, synchronous phase $\phi_s = 30^\circ$,
- 6092 - particle invariant $\varepsilon_Z/\pi = 10^{-6}$ m.

6093 The initial rigidity is taken a few hundred turns upstream of the resonance, namely,
 6094 $B\rho_{\text{ref}} = 4.0880774$ T m, 605226550 MeV, $G\gamma = 2.94931241$, a distance to $G\gamma_R$ of

6095 $4 - \nu_Z - 2.949312415 \approx 0.16223$. Tracking extends a few thousand turns beyond
 6096 $G\gamma_R$ so that S_Z reaches its asymptotic value, from which the resonance strength $|\epsilon_R|$
 6097 can be calculated, using Eq. 17.15.

6098 The simulation file is given in Tab. 17.58. Note the new setting of the SCALING
 6099 factor SCL: DIPOLE field was set for a curvature radius $\rho_0 = 8.4193$ m, given a
 6100 reference rigidity $B\rho_{\text{ref}} \equiv BORO = 0.274426548$ Tm (Tab. 17.46). However the
 6101 reference rigidity is now changed to $B\rho_{\text{ref}} = 4.0880774$ T m, thus maintaining ρ_0
 6102 requires scaling the field in DIPOLE by $4.0880774/0.274426548 = 14.8968$ at turn
 6103 1: this is the new factor, $SCL = 14.8968$, under SCALING (Tab. 17.58). Option
 6104 NT=-1 under SCALING ensures that the scaling factor will automatically follow,
 6105 turn-by-turn, the rigidity boost by CAVITE so preserving constant curvature radius
 6106 $\rho_0 = 8.4193$ m.

6107 The resulting turn-by-turn spin motion is displayed in Fig. 17.67. The Fresnel
 6108 integral model (Eq. 9.41) has been superimposed. Parameters in the latter are as
 6109 follows:

- 6110 - crossing speed $\alpha = \frac{1}{2\pi} \frac{\Delta E}{M} = \frac{1}{2\pi} \frac{10^5 \times \sin 30^\circ [\text{eV/turn}]}{938.27208 \times 10^6 [\text{eV}]} = 8.4812 \times 10^{-6}$,
 - asymptotic $S_{Zf} = 0.999780$, whereas initial $S_{Zi} = 1$, thus (Eq. 17.15)

$$|\epsilon_R|^2 = 5.939 \times 10^{-10}$$

- 6111 - orbital angle origin set at the location of $G\gamma_R$, which is turn 1699.

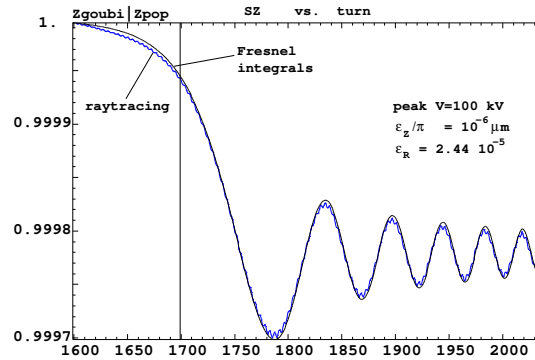


Fig. 17.67 Turn-by-turn spin motion through the isolated resonance $G\gamma_R = 4 - \nu_Z$, case of weak resonance strength. Modulated curve (blue): from raytracing. Smooth curve (black): Fresnel integral model

Table 17.58 Simulation input data file: track a particle launched on a vertical invariant $\varepsilon_y/\pi = 10^{-6}$ m, with horizontal motion indifferent, taken zero here. The INCLUDE adds the SATURNEI cell four times, the latter is defined in Tab. 17.48 and Fig. 9.22

```

SATURNE I ring. Crossing Ggamma=4-nu_Z, weak resonance case (small vertical invariant)
'MARKER' SatIWeakXing_S ! Just for edition purposes.
'OBJET'
4.08897740024e3 ! Reference Brho: 605226550 MeV proton.
8 ! Create a (set of) particle(s) on a given invariant.
1 1 1 ! create a single particle.
0. 0. 0. 0. 0. 1.
0. 14.426 0 ! Horizontal invariant is null.
0. 11.411 1e-6 ! Periodic alpha_Z, beta_Z, and invariant value.
0. 1. 0. ! No momentum spread.
'PARTICUL'
PROTON ! Necessary data in order to allow (i) spin trackingand, and (ii) acceleration.
'SPNTRK' ! Switch on spin tracking,
3 ! nitial spin vertical.
'FAISCEAU'
'FAISTORE'
xing4-Qy.fai ! Log particle data in xing.fai, turn-by-turn.
1

'SCALING'
1 1
DIPOLE
-1 ! Causes field increase in DIPOLE to follow rigidity increase by CAVITE.
14.8968 ! Relative rigidities at turn 1.
1

! 4 cells follow.
'INCLUDE'
1
4* ./SatI_cell.inc[S_SatI_cell:E_SatI_cell]

'CAVITE'
3
0 0
200e3 0.523598775598 ! Acceleration rate is 200*0.5=100keV/turn.

'REBELOTE'
3999 0.3 99 ! A total of 3999+1=4000 turns.

'FAISCEAU'
'MARKER' SatIWeakXing_E ! Just for edition purposes.
'SPNPRT'

'END'

```

6112 (h) Stationary spin motion near a resonance

6113 The simulation input data file of Tab. 17.58 can be used for these fixed energy
6114 trials, with some changes, as follows:

6115 - OBJET[KOBJ=1] is used as it allows to define a set of particles with sampled
6116 momentum offset, namely:

```

6117 'OBJET'
6118 4.4393621786553803e3 ! BORO taken as close to resonant G.gamma as prior knowledge of nu_Z allows.
6119 1 ! Create a set of particles.
6120 1 1 1 1 1 41 ! 41 particles sampling a
6121 0. 0. 0. 0. 0. .00001 ! momentum offset, in -20*1e-5< D-1 < 20*1e-5.
6122 0. 0. 3. 0. 0. 1. ! All particles have initial Z=3cm.
6123

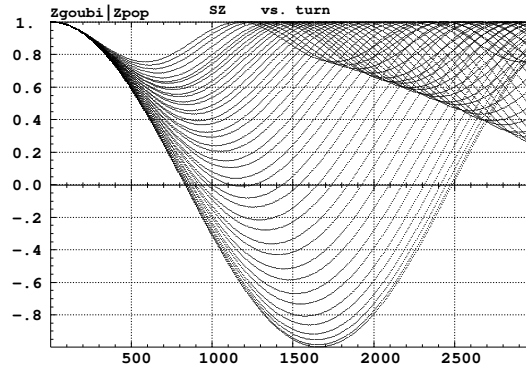
```

6124 - with BORO changed, closer to $G\gamma_R = 4 - \nu_y \approx 3.1115$, DIPOLE field needs to
6125 be set to 5.27284 kG,

6126 - a number of turns $IPASS \approx$ a few thousand, under REBELOTE, results in at least
6127 half an oscillation of $S_Z(\text{turn})$ (the precession frequency increases with the distance
6128 to the resonance, with a minimum of $\omega = |\varepsilon_R|$ on the resonance [8, Fig. 3.4]), which
6129 is convenient for determining $\langle S_Z \rangle$.

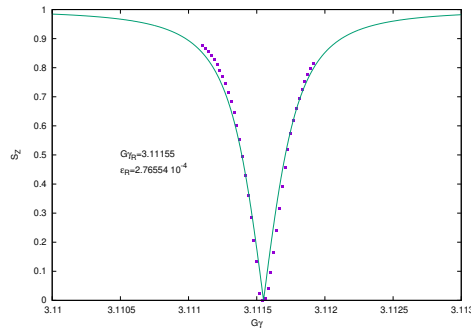
6130 Figure 17.68 displays the turn-by-turn evolution of the vertical component of the
6131 spins as they precess around the eigenvector \mathbf{n} (Eq. 9.20). A quick, and ac-

Fig. 17.68 Turn-by-turn value of the vertical component of spins precessing at fixed energy in SATURNE I synchrotron, observed at the beginning of the sequence, where spins start vertical ($S_Z = 1$). The greater (respectively smaller) the distance to the resonance, the closer the precession axis is to the vertical (resp., to the bend plane), and the greater (resp. the smaller) the oscillation frequency $\omega = \sqrt{\Delta^2 + |\epsilon_R|^2}$



6132 curate enough, approximation to the vertical component of the precession axis
 6133 is $\langle S_Z \rangle_{\text{period}} = \frac{1}{2} \{ \min [S_Z(\theta)] + \max [S_Z(\theta)] \}$, it yields the $\langle S_Z \rangle (\Delta)$ graph of Fig. 17.69.

Fig. 17.69 Vertical component of the spin precession axis as a function of $G\gamma$, in the vicinity of the resonance. Markers are from tracking, solid curve and numerical values of $G\gamma_R$ and ν_Z are from a match using Eq. 9.37



6134 A match of the $\langle S_Z \rangle$ values by (Eq. 9.37)

$$S_y(\Delta) = \frac{\Delta}{\sqrt{\Delta^2 + |\epsilon_R|^2}}$$

given $G\gamma_R = 4 - \nu_Z$, yield vertical tune and resonance strength values, respectively,

$$\nu_Z = 0.88845 \quad \text{and} \quad |\epsilon_R| = 2.77 \times 10^{-4}$$

6135 Satisfactorily, ν_Z is consistent with earlier results, and $|\epsilon_R| = 2.77 \times 10^{-4}$ for $\epsilon_Z/\pi =$
 6136 79×10^{-6} here, is consistent in order of magnitude with $|\epsilon_R| = 2.44 \times 10^{-5}$ for
 6137 $\epsilon_Z/\pi = 10^{-6}$ in the previous question (h). The difference deserves further inspection,
 6138 a possible additional question in this exercise.

6139 (i) Bunch depolarization.

Spin depolarizing resonances in SATURNE I synchrotron are located at (Figs. 17.70, 17.71)

$$G\gamma_R = k \pm \nu_Z = k \pm 0.888284 \quad \equiv 4 - 0.888284, 4 + 0.888284, 8 - 0.888284$$

6140 where ν_Z has been taken from Tab. 17.51, or from Fig. 17.64. $G\gamma_R$ is bounded by
6141 $G\gamma(3\text{ GeV}) = 7.525238 < 8 + \nu_Z$

6142 The simulation data file to track through these resonances is the same as in
6143 question (e), Tab. 17.55, except for the following:

- 6144 - substitute MCOBJET (to be uncommented) to OBJJET (to be commented),
- 6145 - under CAVITE substitute a peak voltage $V = 20\text{ kV}$ to $V = 200\text{ kV}$,
- under REBELOTE, request a 300,000 turn cycle rather than 30,000.

MCOBJET creates a 200 particle bunch with Gaussian transverse and longitudinal densities, with the following *rms* values at 3.6 MeV:

$$\varepsilon_Y/\pi = 25\ \mu\text{m}, \quad \varepsilon_Z/\pi = 10\ \mu\text{m}, \quad \frac{dp}{p} = 10^{-4}$$

6146 CAVITE accelerates that bunch from 3.6 MeV to 3 GeV at a rate of $q\hat{V} \sin(\phi_s) =$
6147 10 keV/turn ($\hat{V} = 20\text{ kV}$, $\phi_s = 30^\circ$), in 300,000 turns.

6148 Figure 17.70 shows sample S_Z spin components of a few particles taken among
6149 the 200 tracked. Figure 17.71 displays $\langle S_Z \rangle$, the vertical polarization component of
6150 the 200 particle set. A gnuplot script is used, given in Tab. 17.59.

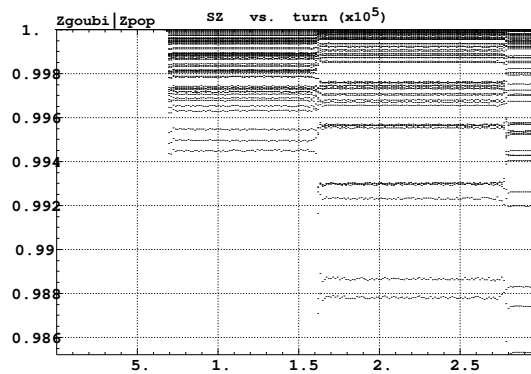


Fig. 17.70 Vertical spin component of a few particles accelerated from 3.6 MeV to 3 GeV. A graph obtained using zpop, data read from [b_]zgoubi.fai: menu 7; 1/2 to open b_zgoubi.fai; 2/[20,23] for S_Z versus turn; 7 to plot

6151 The strength of any one of the three resonances crossed can be computed, from
6152 the upstream and downstream bunch polarization averaged over the 200 particles,
6153 using Eq. 17.15. Dependence upon the vertical emittance of the bunch can be
6154 performed repeating this tracking simulation, with a different vertical emittance
6155 (under MCOBJET).

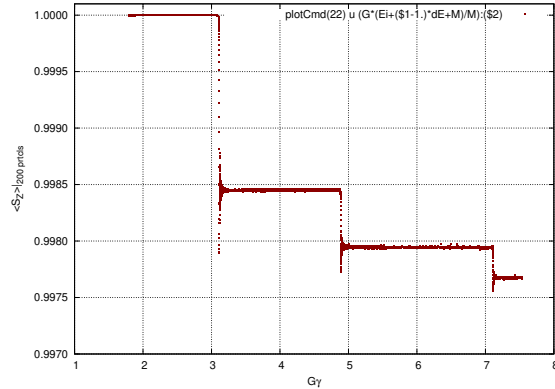


Fig. 17.71 Average vertical spin component of a 200 particle bunch, accelerated from 3.6 MeV to 3 GeV

Table 17.59 A gnuplot script to plot the average vertical spin component of the 200 particle set, along the acceleration ramp (Fig. 17.71). The average is prior computed by an awk script, which reads the necessary data from zgoubi.fai.

```
# gnuplot_avrgFromFai.gnu
fname = 'zgoubi.fai'; plotCmd(col_num)=sprintf('< gawk -f average.awk -v col_num=%d %s', col_num, fname)
set xtics; set ytics; set xlabel "G/(Symbol g)"; set ylabel "<S_Z>|_{200 prtcls}"
set format y '%0.4f'; set grid; set xr [:]; set yr [.997:1.0001]
Qy=0.888248;
do for [intgr=1:2] { set arrow nohead from 4*intgr-Qy, 0.997 to 4*intgr-Qy, 1.0001 lw 1 dt 2
set arrow nohead from 4*intgr+Qy, 0.997 to 4*intgr+Qy, 1.0001 lw 1 dt 2 }
M=938.27208; Ei = 3.6; G = 1.79284735; Qy = 0.888284; dE = 0.01 # MeV/turn
plot plotCmd(22) u (G*(Ei+(S1-1.)*dE+M)/M):(S2) w p pt 5 ps .4 lc rgb 'dark-red'; pause 1
```

average.awk script to compute $\langle S_Z \rangle$ [5]:

```
function average(x, data){
  n = 0; mean = 0;
  val_min = 0; val_max = 0;
  for(val in data){
    n += 1;
    delta = val - mean;
    mean += delta/n;
    val_min = (n == 1)?val:((val < val_min)?val:val_min);
    val_max = (n == 1)?val:((val > val_max)?val:val_max);
  }
  if(n > 0){
    print x, mean, val_min, val_max;
  }
}
{
  curr = $38;
  yval = $(col_num);

  if(NR==1 || prev != curr){
    average(prev, data);
    delete data;
    prev = curr; }
  data[yval] = 1; }
END{
  average(curr, data); }
```

6156 Checking dependence upon crossing speed of the depolarizing effect of the res-
 6157 onances can be performed by repeating this tracking simulation with a different
 6158 accelerating rate $\dot{V} \sin(\phi_s)$.